Journal of Applied Polymer Science

Measurement of Concentration Profiles Using Confocal Raman Spectroscopy in Multicomponent Polymeric Coatings—Model Validation

Raj Kumar Arya,[1] Madhu Vinjamur[2]

[1]Department of Chemical Engineering, Jaypee University of Engineering & Technology, Guna, Raghogarh, Guna 473226, Madhya Pradesh, India

[2]Department of Chemical Engineering, Indian Institute of Technology Bombay, Powai 400076, Mumbai, India

Correspondence to: R. K. Arya (E-mail: raj.arya@juet.ac.in)

ABSTRACT: Concentrations of the solvents were measured using confocal laser Raman Spectroscopy for two ternary systems, poly(styrene)—tetrahydrofuran—*p*-xylene and poly(methyl methacrylate)—ethylbenzene—tetrahydrofuran, during drying at room temperature. The concentrations were compared with predictions of drying models, which utilize several existing theories for mutual diffusion coefficients for polymer solvent systems. Of the nine free volume parameters required to predict diffusion coefficients of binary systems, four for each of the four pairs studied here were estimated as suggested by the literature. Estimation was done by minimizing the difference between predictions of the model and experimental weight loss data for each binary pair. It is found that the predictions of the models which include cross term diffusion coefficients are in better agreement with measured concentrations than those which ignore the cross terms. © 2012 Wiley Periodicals, Inc. J. Appl. Polym. Sci. 128: 3906–3918, 2013

KEYWORDS: coatings; diffusion; Raman spectroscopy; thin films

Received 3 May 2011; accepted 17 September 2012; published online 16 October 2012
DOI: 10.1002/app.38589

INTRODUCTION

Many homogeneous and dense polymeric coatings are made by drying thin films cast from solutions of one polymer dissolved in two or more solvents. Multicomponent systems offer several advantages such as ability to dissolve polymer, control of drying rates and use of cheaper solvents.[1] Asymmetric membranes, having thin and dense upper layer and thick and porous bottom layer, were produced by drying of ternary systems consisting of a polymer, a solvent and a nonsolvent.[2–6] Such membranes could be also made by dissolving a solution of a polymer in a solvent and in a nonsolvent. The nonsolvent diffuses into the solution and the solvent diffuses out of the solution leading to phase separation. Diffusion is central to description of drying processes of homogeneous and heterogeneous coatings as internal diffusion controls the drying rate for most part of drying.

In binary polymer solvent systems, solvent diffuses due to its own concentration gradient and, one mutual diffusion coefficient describes the transport. The rate of change of solvent concentration at a point equals the gradient of flux there.

$$\frac{\partial c}{\partial t} = \frac{\partial}{\partial z}\left(D(c,T)\frac{\partial c}{\partial z}\right) \tag{1}$$

c is concentration of the solvent, t is time, z is distance, and D is mutual diffusion coefficient, which is a strong function of concentration and temperature, T.

D is predicted accurately for many polymer solvent systems by Vrentas and Duda free volume theory[7,8] in conjunction with Flory-Huggins theory for polymer solution thermodynamics. Many parameters are needed for prediction of the mutual diffusion coefficient; these have been documented by Hong[9] for several polymers and solvents. Diffusion coefficients predicted by the above theory have been used extensively in drying models. The results of these models compare well with experimental weight loss data.[10–12] Recently, the results of the models have been shown to compare well with depth profile measurements using confocal laser Raman spectroscopy.[13]

In multicomponent systems, a solvent diffuses due to its own concentration gradient and those of other solvents also.[14–16] For

a N-component system consisting of one polymer and $(N-1)$ solvents, the rate of change of concentration of the solvents is given by the following matrix equation:

$$\begin{bmatrix} \frac{\partial c_1}{\partial t} \\ \frac{\partial c_2}{\partial t} \\ . \\ . \\ . \\ \frac{\partial c_{N-1}}{\partial t} \end{bmatrix} = \begin{bmatrix} D_{11} D_{12} \ldots D_{1,N-1} \\ D_{21} D_{22} \ldots D_{2,N-1} \\ \ldots\ldots\ldots\ldots \\ \ldots\ldots\ldots\ldots \\ \ldots\ldots\ldots\ldots \\ D_{N-1,1} D_{N-1,2} \ldots D_{N-1,N-1} \end{bmatrix} \begin{bmatrix} \frac{\partial c_1}{\partial z} \\ \frac{\partial c_2}{\partial z} \\ . \\ . \\ . \\ \frac{\partial c_{N-1}}{\partial z} \end{bmatrix} \quad (2)$$

D_{ii} are called main-term diffusion coefficients and others are called cross-term diffusion coefficients.

Several theories for predicting the main-term and the cross-term diffusion coefficients have appeared in the literature. The theories begin with Bearman's statistical mechanical theory[17] that relates gradient of chemical potential of a species to frictional motion between the species and others of the system.

$$\frac{\partial \mu_i}{\partial z} = -\sum_{j=1}^{n} \frac{c_j}{M_j} \xi_{ij} (v_i - v_j) \quad (3)$$

$\frac{\partial \mu}{\partial z}$ is chemical potential gradient, c_j, local mass concentration of component j, M_j is molecular weight of component j, ξ_{ij} is friction coefficient between component i and j, v_i & v_j are the mean velocities of component i and j respectively

According to Bearman, self-diffusion coefficients are also related to friction is given by

$$D_i = \frac{RT}{\sum_{J=1}^{n} \frac{c_j}{M_j} \xi_{ij}} \quad (4)$$

D_i is self-diffusion coefficient of species i, M_j is molecular weight of component j, R is universal gas constant and T is absolute temperature. Friction factors ξ_{ij} cannot be measured directly. Different assumptions on them led to different theories for diffusion in multicomponent mixtures.

Zielinski and Hanley[18] assumed modeled gradient of chemical potential due to average force experienced by a molecule. They related mass flux of a species expressed relative to mass average velocity to the gradient of chemical potential and developed a model for the main-term and the cross-term coefficients. The model equations, shown below, were derived for ternary polymer solvent systems; the equations could easily be extended to N-component system.

$$D_{11} = D_1 c_1 (1 - c_1 \hat{V}_1 + c_1 \hat{V}_3) \left[\frac{\partial \ln a_1}{\partial c_1}\right] + D_2 c_1 c_2 (\hat{V}_3 - \hat{V}_2) \left[\frac{\partial \ln a_2}{\partial c_1}\right] \quad (5)$$

$$D_{12} = D_1 c_1 (1 - c_1 \hat{V}_1 + c_1 \hat{V}_3) \left[\frac{\partial \ln a_1}{\partial c_2}\right] + D_2 c_1 c_2 (\hat{V}_3 - \hat{V}_2) \left[\frac{\partial \ln a_2}{\partial c_2}\right] \quad (6)$$

$$D_{21} = D_2 c_2 (1 - c_2 \hat{V}_2 + c_2 \hat{V}_3) \left[\frac{\partial \ln a_2}{\partial c_1}\right] + D_1 c_1 c_2 (\hat{V}_3 - \hat{V}_1) \left[\frac{\partial \ln a_1}{\partial c_1}\right] \quad (7)$$

$$D_{22} = D_2 c_2 (1 - c_2 \hat{V}_2 + c_2 \hat{V}_3) \left[\frac{\partial \ln a_2}{\partial c_2}\right] + D_1 c_1 c_2 (\hat{V}_3 - \hat{V}_1) \left[\frac{\partial \ln a_1}{\partial c_2}\right] \quad (8)$$

c_i is concentration of solvent i $(i = 1, 2)$, V is specific volume of solvent i, a_i is activity of solvent i and D_i is self-diffusion coefficient of solvent i.

Dabral[19] developed multicomponent diffusion models for polymer –solvent-solvent system assuming that solvent-solvent friction factors (ξ_{11}, ξ_{12}, ξ_{22}, ξ_{21}) were negligible compared to polymer–solvent friction factor (ξ_{13} & ξ_{23}). The developed equations for the diffusion coefficients are:

$$D_{11} = D_1 c_1 (1 - c_1 \hat{V}_1) \left[\frac{\partial \ln a_1}{\partial c_1}\right] - D_2 c_1 c_2 \hat{V}_2 \left[\frac{\partial \ln a_2}{\partial c_1}\right] \quad (9)$$

$$D_{12} = D_1 c_1 (1 - c_1 \hat{V}_1) \left[\frac{\partial \ln a_1}{\partial c_2}\right] - D_2 c_1 c_2 \hat{V}_2 \left[\frac{\partial \ln a_2}{\partial c_2}\right] \quad (10)$$

$$D_{21} = D_2 c_2 (1 - c_2 \hat{V}_2) \left[\frac{\partial \ln a_2}{\partial c_1}\right] - D_1 c_1 c_2 \hat{V}_1 \left[\frac{\partial \ln a_1}{\partial c_1}\right] \quad (11)$$

$$D_{22} = D_2 c_2 (1 - c_2 \hat{V}_2) \left[\frac{\partial \ln a_2}{\partial c_2}\right] - D_1 c_1 c_2 \hat{V}_1 \left[\frac{\partial \ln a_1}{\partial c_2}\right] \quad (12)$$

Alsoy and Duda[20] presented models for diffusion coefficients for four cases. In one case, the ratio of friction factors was assumed to be constant; in another case, the cross-term coefficients were set to zero; in yet another case, the cross-term coefficients were set to zero and the main-term coefficients were set equal to self-diffusion coefficients; in still another case, the friction factors were set to zero. Detailed derivation of the diffusion coefficients is available in Alsoy.[21] Table I shows the diffusion coefficients for all the four cases. Equations of Case 4 are same as those of Dabral.[19]

Zielinski and Alsoy[22] checked the consistency of multicomponent diffusion models using Onsager relations. They showed that Zielinski and Hanley[18] model satisfies the Onsager relation for low molecular weight species but fails for higher molecular weight species. Alsoy and Duda[20] models were also unable to satisfy the Onsager relations. In case 1, ratio of friction factors was assumed constant and equal to the partial molar volumes of components which cannot hold throughout the concentration range. In case 4, friction coefficients between the diffusing components was assumed to be zero which gives ratio of friction factor between the solvent and solute equal to the ratio of their self-diffusion coefficient. According to Bearman's theory, friction factor between the components is inversely proportional to the self-diffusion coefficient. Therefore, this model satisfied the Onsager relations.

Nauman and Savoca[23] have reported that concentration for the balancing component could become negative if the ratio of

Table I. Four Cases for Diffusion Coefficients of Ternary Polymer Solvent Systems[20]

Case	D_{11}	D_{12}	D_{21}	D_{22}
1	$D_1\left[\frac{\partial \ln a_1}{\partial \ln c_1}\right]$	$\frac{c_1}{c_2}D_1\left[\frac{\partial \ln a_1}{\partial \ln c_2}\right]$	$\frac{c_2}{c_1}D_2\left[\frac{\partial \ln a_2}{\partial \ln c_1}\right]$	$D_2\left[\frac{\partial \ln a_2}{\partial \ln c_2}\right]$
2	$D_1\left[\frac{\partial \ln a_1}{\partial \ln c_1}\right]$	0	0	$D_2\left[\frac{\partial \ln a_2}{\partial \ln c_2}\right]$
3	D_1	0	0	D_2
4	$D_1c_1(1-c_1\hat{V}_1)\left[\frac{\partial \ln a_1}{\partial c_1}\right] - D_2c_1c_2\hat{V}_2\left[\frac{\partial \ln a_2}{\partial c_1}\right]$	$D_1c_1(1-c_1\hat{V}_1)\left[\frac{\partial \ln a_1}{\partial c_2}\right] - D_2c_1c_2\hat{V}_2\left[\frac{\partial \ln a_2}{\partial c_2}\right]$	$D_2c_2(1-c_2\hat{V}_2)\left[\frac{\partial \ln a_2}{\partial c_1}\right] - D_1c_1c_2\hat{V}_1\left[\frac{\partial \ln a_1}{\partial c_1}\right]$	$D_2c_2(1-c_2\hat{V}_2)\left[\frac{\partial \ln a_2}{\partial c_2}\right] - D_1c_1c_2\hat{V}_1\left[\frac{\partial \ln a_1}{\partial c_2}\right]$

diffusion coefficients is constant during the transport. During the course of drying, diffusivities change by several orders of magnitude; therefore, the assumption of constant diffusivities will lead to negative concentration for the polymer.

Price and Romdhane[24] presented a generalized theory, again based on Bearman's friction theory, which unifies the above models. They defined ratio of friction coefficients as $\frac{\xi_{ij}}{\xi_{ik}}=\frac{\alpha_j\overline{V_j}}{\alpha_k\overline{V_k}}=\frac{\alpha_j\hat{V}_j\ M_j}{\alpha_k\hat{V}_k\ M_k}$, where α is a constant. Using this ratio, they derived equations for diffusion coefficients which are shown below.

$$D_{11}=\left[1-c_1\hat{V}_1\left(1-\frac{\alpha_1}{\alpha_3}\right)\right]c_1D_1\frac{\partial \ln a_1}{\partial c_1}-\left(1-\frac{\alpha_2}{\alpha_3}\right)c_2\hat{V}_2c_1D_2\frac{\partial \ln a_2}{\partial c_1} \quad (13)$$

$$D_{12}=\left[1-c_1\hat{V}_1\left(1-\frac{\alpha_1}{\alpha_3}\right)\right]c_1D_1\frac{\partial \ln a_1}{\partial c_2}-\left(1-\frac{\alpha_2}{\alpha_3}\right)c_2\hat{V}_2c_1D_2\frac{\partial \ln a_2}{\partial c_2} \quad (14)$$

$$D_{21}=\left[1-c_2\hat{V}_2\left(1-\frac{\alpha_2}{\alpha_3}\right)\right]c_2D_2\frac{\partial \ln a_2}{\partial c_1}-\left(1-\frac{\alpha_1}{\alpha_3}\right)c_1\hat{V}_1c_2D_1\frac{\partial \ln a_1}{\partial c_1} \quad (15)$$

$$D_{22}=\left[1-c_2\hat{V}_2\left(1-\frac{\alpha_2}{\alpha_3}\right)\right]c_2D_2\frac{\partial \ln a_2}{\partial c_2}-\left(1-\frac{\alpha_1}{\alpha_3}\right)c_1\hat{V}_1c_2D_1\frac{\partial \ln a_1}{\partial c_2} \quad (16)$$

All other previous models[18–20] are some special cases of generalized model.[24] By setting different values to α_i, the theories can be recovered.

For Dabral[19] model, $\alpha_i=0,\ i\neq N$

For Zielinski and Hanley[18] model, $\alpha_i=\frac{1}{\hat{V}_i},\ i=1,.....N$

For Alsoy and Duda[20] model, $\alpha_i=1,\ i=1,.....N$

In generalized model, ratio of self-diffusion coefficients were set equal to ratio of friction factors, $\frac{\xi_{ij}}{\xi_{ik}}=\frac{\alpha_j\overline{V_j}}{\alpha_k\overline{V_k}}=\frac{\alpha_j\hat{V}_jM_j}{\alpha_k\hat{V}_kM_k}=\frac{D_k}{D_j},\ j\neq i,\ i,k=1,.....N-1$

The generalized diffusion equations predicted by them are following

$$D_{11}=c_1c_2\hat{V}_2\left(D_1\frac{\partial \ln a_1}{\partial c_1}-D_2\frac{\partial \ln a_2}{\partial c_1}\right)+c_1c_3\hat{V}_3\left(D_1\frac{\partial \ln a_1}{\partial c_1}-D_3\frac{\partial \ln a_3}{\partial c_1}\right) \quad (17)$$

$$D_{12}=c_1c_2\hat{V}_2\left(D_1\frac{\partial \ln a_1}{\partial c_2}-D_2\frac{\partial \ln a_2}{\partial c_2}\right)+c_1c_3\hat{V}_3\left(D_1\frac{\partial \ln a_1}{\partial c_2}-D_3\frac{\partial \ln a_3}{\partial c_2}\right) \quad (18)$$

$$D_{21}=c_2c_1\hat{V}_1\left(D_2\frac{\partial \ln a_2}{\partial c_1}-D_1\frac{\partial \ln a_1}{\partial c_1}\right)+c_2c_3\hat{V}_3\left(D_2\frac{\partial \ln a_2}{\partial c_1}-D_3\frac{\partial \ln a_3}{\partial c_1}\right) \quad (19)$$

$$D_{22}=c_2c_1\hat{V}_1\left(D_2\frac{\partial \ln a_2}{\partial c_2}-D_1\frac{\partial \ln a_1}{\partial c_2}\right)+c_2c_3\hat{V}_3\left(D_2\frac{\partial \ln a_2}{\partial c_2}-D_3\frac{\partial \ln a_3}{\partial c_2}\right) \quad (20)$$

The generalized theory requires self-diffusion coefficient of the polymer—a shortcoming of the theory because few experimental data are available for this coefficient. Activity of the solvents for the ternary polymer–solvent–solvent system can be calculated using Flory Huggins theory. The equations for the activities are given in next section.

Accurate description of transport in multicomponent systems requires precise values for both the coefficients. There are a few reports on experimental measurements of self-diffusion coefficients in ternary polymer solvent systems. Surana et al.[25] reported measurements of self-diffusion coefficient of a trace of a second solvent in polymer–first solvent–second solvent systems using inverse gas chromatography (IGC). They showed

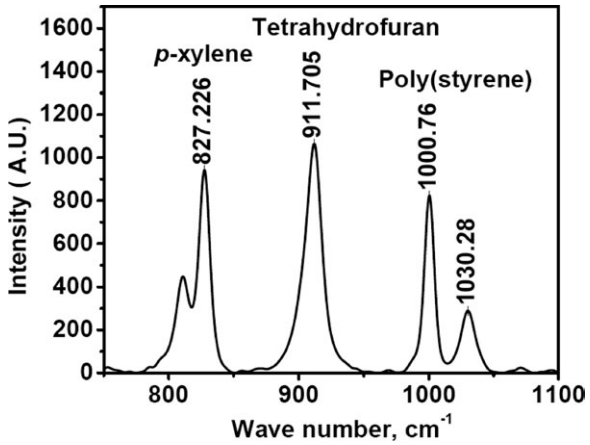

Figure 1. Raman spectra of poly (styrene)–tetrahydrofuran–*p*-xylene ternary system.

that the measurements compare reasonably well with the predictions of free volume theory. Galdamez and Danner[26] developed a new and simplified model to describe diffusion in ternary polymer solvent systems and compared the model predictions with IGC measurements. They concluded that the cross-term diffusion coefficients were negligible for the system they considered but, the thermodynamic cross-terms were not. Measurements with IGC are also limited to low concentrations of solvents. Muller et al.[27] reported diffusion coefficients of a nonvolatile plasticizer in solutions of poly(vinyl acetate) in methylene chloride. The experimental measurements report self-diffusion coefficients over a narrow range.

It is unclear which of the theoretical models describes transport accurately in multicomponent polymer solvent systems. Testing the predictions of diffusion coefficients by the models against experimental data is the best way to assess them. However, few experimental data for the main-term coefficients are available and it is difficult to measure the cross-term coefficients. Price and Romdhane[24] have also raised questions on the applicability of Flory-Huggins theory for multicomponent polymer solvent systems. In this work, the above-mentioned theories are rigorously tested by comparing predictions of drying model, which utilizes the theories for diffusion coefficients, with measurements of solvent concentration as a function of time and distance in drying ternary coatings using confocal laser Raman spectroscopy.

MATERIALS AND METHODS

In this study, ternary systems consisting of one polymer and two solvents have been considered. The systems chosen for the study were: poly(styrene)-tetrahydrofuran–*p*-xylene and poly(methyl methacrylate)–tetrahydrofuran – ethylbenzene. Figures 1 and 2 show that for both the systems, the components have well separated characteristic peaks, thus the components can be differentiated during analysis by confocal Raman spectroscopy. For example, *p*-xylene shows a peak at a wave number of about 827 cm^{-1}, tetrahydrofuran at 911 cm^{-1}, poly(styrene) at 1000 cm^{-1}, poly(methyl methacrylate) at 810 cm^{-1} and ethylbenzene at 1001 cm^{-1}. Chow[28] has studied the effects of diluents on poly(styrene) glass transition temperature. This study suggests that glass transition temperature of poly(styrene) will be around 31°C for 10 w% tetrahydrofuran solution. Ternary systems studied here have higher amount of diluents during the course of drying. Hence both the ternary systems will remain rubbery during drying and may reach to glass transition temperature only at the end of drying due to solvent loss. The properties and suppliers of materials used are listed in Table II.

EXPERIMENTAL

Two procedures are explained below. One is for calibration and the other is for measurement of concentrations during drying of a ternary polymer solution. Calibration procedure is given by Arya.[29]

Figure 3–6 show calibration plots for poly(styrene)-tetrahydrofuran, poly(styrene)–*p*-xylene, poly(methyl methacrylate)–tetrahydrofuran and poly(methyl methacrylate)–ethylbenzene.[29] Binary calibration plots were used to calculate concentration of solvents and polymer in ternary systems.

Procedure for Measurement of Concentrations Using Confocal Laser Raman Spectroscopy

1. An empty sample holder was kept on a platform below the objective and the base of the holder was located.
2. Video of the base of the sample holder was viewed to confirm the position of the base. Also, spectra (20×, dry objective) at the base was taken, which was completely noisy.
3. Exact volume of the polymer solution was injected into the sample holder with a micropipette stop watch was started. Internal diameter and depth of sample holder were 12 mm and 1 mm, respectively and, injected volume was 155 μL. For 14.17 wt % poly (styrene)—70.15 wt % tetrahydrofuran—15.68 wt % *p*-xylene system an injected volume of 155 μL resulted in a coating with a thickness of 1004 μm. For 19.71 wt % poly (methyl methacrylate)—70.56 wt % tetrahydrofuran—9.71 wt % ethylbenzene system an injected volume of 150 μL resulted in a coating with a thickness of 983 μm. Thirty samples were weighed for each system to calculate the initial thickness; an

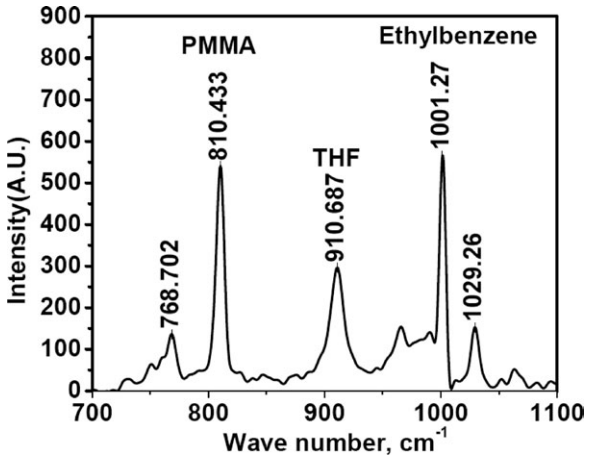

Figure 2. Raman spectra of poly (methyl methacrylate)–tetrahydrofuran–ethylbenzene ternary system.

Table II. Specifications of Materials Used

Name of chemical	Supplier	Molecular weight, g . mol^{-1}	Density g . cm^{-3}	Refractive index
Poly (styrene)	Sigma Aldrich, Germany	230000	1.047	1.46
Poly (methyl methacrylate)	Sigma Aldrich, Germany	120000	1.188	1.497
Tetrahydrofuran	Qualigens Fine Chemicals, India	72.11	0.886	1.407
Ethylbenzene	Spectrochem Pvt. Ltd., India	106.17	0.886	1.495
p-Xylene	S.D.Fine-Chem Ltd., India	106.17	0.861	1.4950

average thickness is reported here. Average weight and standard deviation for weight measurement experiments for poly (styrene) case were 0.1028 g and 0.0016 g, respectively and those for poly (methyl methacrylate) case were 0.1050 g and 0.0014 g, respectively.

4. Again locate the base quickly.
5. Adjust the depth of penetration to the desired value at certain time and take the spectra.
6. Calculate the ratios of Raman intensities of the polymer to the solvent for given sample and find the concentration of each component using binary calibration plots.

Binary calibration plots were used to calculate concentration of solvents and polymer in ternary systems. For given ternary sample, Raman spectra were recorded at several position and time. For particular instance, the ratio of intensities of PS/THF, PS/*p*-xylene, PMMA/EB, and PMMA/THF can be found. Then from the calibration curves, the values of weight ratios of PS/THF, PS/*p*-xylene, PMMA/EB and PMMA/EB are read as shown in following example:

From the Raman spectra one can find

$$\frac{\text{Inetnsity of PS}}{\text{Intensity of } p\text{-xylene}} = 1.7471 \tag{21}$$

$$\frac{\text{Intensity PS}}{\text{Intensity of THF}} = 0.8511 \tag{22}$$

Equations to calibration curves are given as following

$$\frac{\text{g PS}}{\text{g THF}} = 0.4612 \frac{\text{Intensity of PS}}{\text{Intensity of THF}} \tag{23}$$

$$\frac{\text{g PS}}{\text{g } p\text{-xylene}} = 0.6866 \frac{\text{Intensity of PS}}{\text{Intensity of } p\text{-xylene}} \tag{24}$$

Let the amount of poly(styrene) be 1 g, then following calculations can be made

From eqs. (21) and (24)

$$\frac{1}{\text{g } p\text{-xylene}} = 0.6866 \times 1.7471 \Rightarrow p\text{-xylene} = 0.8336\, g$$

From eqs. (22) and (23)

$$\frac{1}{\text{g THF}} = 0.4612 \times 0.8511 \Rightarrow \text{THF} = 2.5474\ g$$

Now amounts of poly(styrene), p-xylene, and THF are 1 g, 0.8336 g, and 2.5474 g, respectively. Total volume can be calculated using density of each component.

$$\begin{bmatrix}\text{concentration of} \\ \text{poly(styrene)}\end{bmatrix} = \frac{\text{amount of PS}}{\frac{\text{amount of PS}}{\rho_{\text{PS}}} + \frac{\text{amount of THF}}{\rho_{\text{THF}}} + \frac{\text{amount of } p\text{-xylene}}{\rho_{\text{p-xylene}}}}$$
$$= 0.2084\, g\,.\,\text{cm}^{-3}$$

Similarly concentrations of *p*-xylene and tetrahydrofuran were calculated 0.1737g. cm^{-3}and 0.5308 g . cm^{-3} respectively.

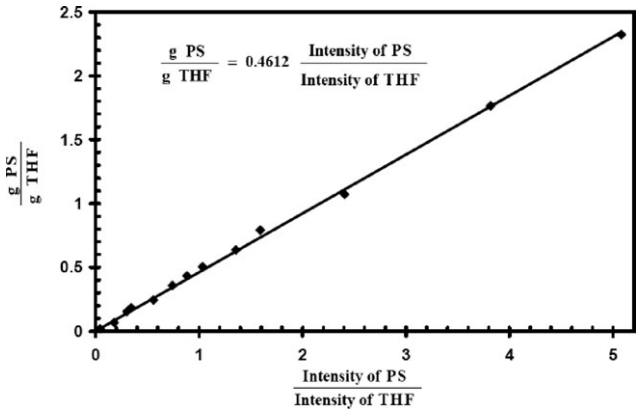

Figure 3. Calibration plot for poly (styrene)–tetrahydrofuran system.

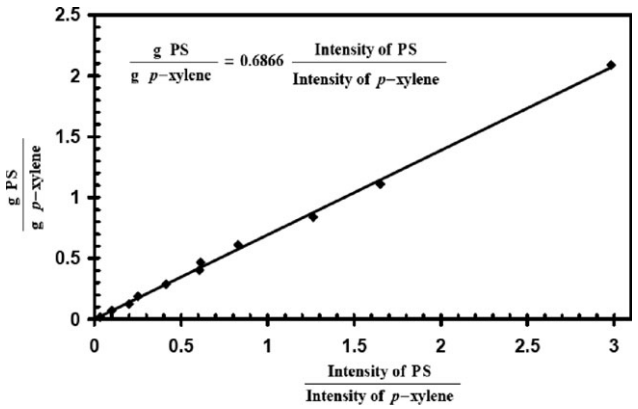

Figure 4. Calibration plot for poly (styrene)–*p*-xylene system.

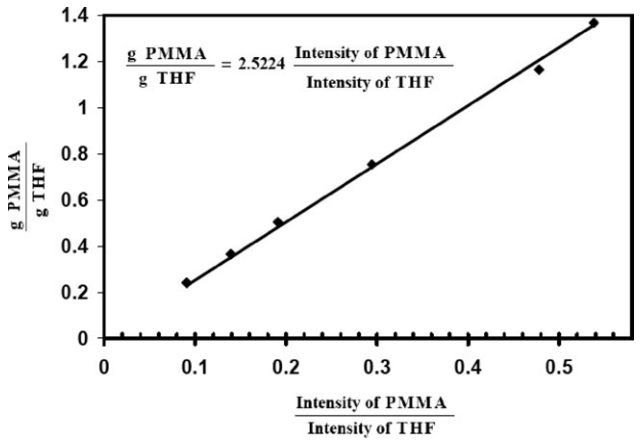

Figure 5. Calibration plot for poly (methyl methacrylate)–tetrahydrofuran system.

GOVERNING EQUATIONS

Figure 7 shows the schematic of a drying ternary coating that has been cast on an impermeable substrate. The solvents move from the bottom to the surface and evaporate into the drying air. As the solvents depart the coating, it shrinks with time. There is no mass transfer through the substrate; hence, flux of both the solvents is zero at the substrate. The coating is heated from both the top and bottom sides.

Mass Balance for Solvent 1:

$$\frac{\partial c_1}{\partial t} = \frac{\partial}{\partial z}\left(D_{11}\frac{\partial c_1}{\partial z}\right) + \frac{\partial}{\partial z}\left(D_{12}\frac{\partial c_2}{\partial z}\right) \tag{25}$$

Mass Balance for Solvent 2:

$$\frac{\partial c_2}{\partial t} = \frac{\partial}{\partial z}\left(D_{21}\frac{\partial c_1}{\partial z}\right) + \frac{\partial}{\partial z}\left(D_{22}\frac{\partial c_2}{\partial z}\right) \tag{26}$$

The reference velocity is chosen to be volume average velocity because it is shown to be zero if there is no change in volume on mixing.[30]

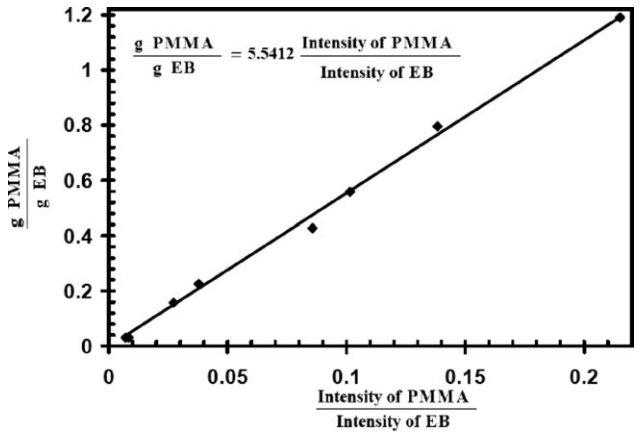

Figure 6. Calibration plot for poly(methyl methacrylate)–ethylbenzene system.

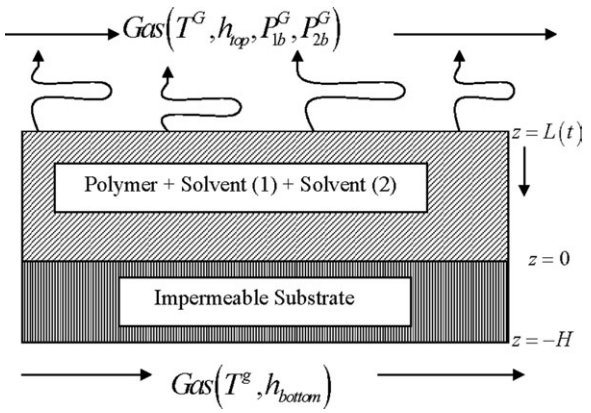

Figure 7. Schematic of a drying coating.

c_i is concentration of solvent i, t is time, z, is thickness of the coatings at anytime, D_{11} and D_{22} are the main-term diffusion coefficients that characterize transport due to solvents own concentration gradient, D_{12} and D_{21} are the cross-term diffusion coefficients that characterize transport due to other solvents concentration gradient.

Mutual diffusion coefficients were calculated using multicomponent diffusion models discussed above. Self-diffusion coefficients were calculated using Vrentas and Duda[7,8] free volume theory:

$$D_i = D_{0i}\exp\left(-\frac{\left(\sum_{j=1}^{3}\omega_j\hat{V}_j^*\frac{\xi_{j3}}{\xi_{j3}}\right)}{\frac{\hat{V}_{FH}}{\gamma}}\right) \tag{27}$$

$\xi_{i3} = \frac{\text{critical molar volume of a jumping unit of component } i}{\text{critical molar volume of the jumping unit of the polymer}} = \frac{\hat{V}_i^* M_{ji}}{\hat{V}_3^* M_{j3}}$ (Vrentas et al.[31]), and

The hole free volume is given by:

$$\frac{\hat{V}_{FH}}{\gamma} = \frac{K_{11}}{\gamma}\omega_1(K_{21}+T-T_{g1}) + \frac{K_{12}}{\gamma}\omega_2(K_{22}+T-T_{g2}) + \frac{K_{13}}{\gamma}\omega_3(K_{23}+T-T_{g3}) \tag{28}$$

Uniform concentration of the solvents throughout the coating are the initial conditions for eqs. (25) and (26). The boundary conditions are described by fluxes at the top and bottom of the coating.

Flux of solvent 1 at the top surface:

$$\left(-D_{11}\frac{\partial c_1}{\partial z} - D_{12}\frac{\partial c_2}{\partial z}\right)\Big|_{z=L(t)} = (1-c_1\overline{V_1})\,k_1^G(p_{1i}^G - p_{1b}^G) - c_1\overline{V_2}\,k_2^G(p_{2i}^G - p_{2b}^G) \tag{29}$$

Flux of solvent 2 at the top surface:

$$\left(-D_{22}\frac{\partial c_2}{\partial z} - D_{21}\frac{\partial c_1}{\partial z}\right)\Big|_{z=L(t)} = (1-c_2\overline{V_2})\,k_2^G(p_{2i}^G - p_{2b}^G) - c_2\overline{V_1}\,k_2^G(p_{1i}^G - p_{1b}^G) \tag{30}$$

k_1^G and k_2^G are the convective mass transfer coefficients for solvents 1 and solvent 2, respectively.

Flux of solvent 1 at the substrate:

$$\left(-D_{11}\frac{\partial c_1}{\partial z} - D_{12}\frac{\partial c_2}{\partial z}\right)|_{z=0} = 0 \tag{31}$$

Flux of solvent 2 at the substrate:

$$\left(-D_{22}\frac{\partial c_2}{\partial z} - D_{21}\frac{\partial c_1}{\partial z}\right)|_{z=0} = 0 \tag{32}$$

Shrinkage of Coating

Coating shrinks due to departure of both the solvents into the room air.

$$\frac{dL}{dt} = -\overline{V_1}k_1^G\left(p_{1i}^G - p_{1b}^G\right) - \overline{V_2}k_2^G\left(p_{2i}^G - p_{2b}^G\right) \tag{33}$$

L is the thickness of coating; $\overline{V}_1$ and $\overline{V}_2$ are the partial molar volume of solvents 1 and 2, respectively; p_{1b}^G and p_{2b}^G are partial pressures of solvents 1 and 2 in bulk air, respectively;

$$p_{1i} = P_1^{\text{vap}}(T).\phi_1.\gamma_1 \tag{34}$$

$$p_{2i} = P_2^{\text{vap}}(T).\phi_2.\gamma_2 \tag{35}$$

γ_1 and γ_2, are the activity constants for the solvent 1 and 2 respectively.

Activity for the ternary systems can be calculated using Flory Huggins theory.[32]

Activity coefficient of solvent 1:

$$\ln a_1 = \ln\gamma_1 + \ln\phi_1 = \ln\phi_1 + \left(1 - \phi_1 - \frac{\overline{V_1}}{\overline{V_2}}\phi_2\right) - \frac{\overline{V_1}}{\overline{V_3}}\phi_3 + \chi_{13}\phi_3^2 + \chi_{12}\phi_2^2 + \phi_2\phi_3\left(\chi_{13} + \chi_{12} - \frac{\overline{V_1}}{\overline{V_2}}\chi_{23}\right) \tag{36}$$

Activity coefficient of solvent 2:

$$\ln a_2 = \ln\gamma_2 + \ln\phi_2 = \ln\phi_2 + \left(1 - \frac{\overline{V_2}}{\overline{V_1}}\phi_1 - \phi_2\right) - \frac{\overline{V_2}}{\overline{V_3}}\phi_3 + \chi_{23}\phi_3^2 + \chi_{12}\frac{\overline{V_2}}{\overline{V_1}}\phi_2^2 + \phi_1\phi_3\left(\chi_{12}\frac{\overline{V_2}}{\overline{V_1}} + \chi_{23} - \frac{\overline{V_2}}{\overline{V_1}}\chi_{13}\right) \tag{37}$$

$$\ln a_3 = \ln\phi_3 + (1-\phi_3) - \frac{\overline{V_3}}{\overline{V_1}}\phi_1 - \frac{\overline{V_3}}{\overline{V_2}}\phi_2 + \left(\chi_{13}\frac{\overline{V_3}}{\overline{V_1}}\phi_1 + \chi_{23}\frac{\overline{V_3}}{\overline{V_2}}\phi_2\right)(\phi_1+\phi_2) - \chi_{12}\frac{\overline{V_3}}{\overline{V_1}}\phi_1\phi_2 \tag{38}$$

Where, χ, is the Flory – Huggins binary interaction parameter can be determined from the Bristow and Watson[33] semiempirical equation given below,

$$\chi_{ij} = 0.35 + \frac{\overline{V}_i}{RT}\left(\delta_i - \delta_j\right)^2 \tag{39}$$

$\overline{V}_i$ is the partial molar volume of solvent i, δ_i is the solubility parameter of solvent i, δ_j is the solubility parameter of polymer j, and volume fraction is given by $\phi_i = c_i\hat{V}_i$, where c_i is the concentration of species i, $\hat{V}_i$ is the specific volume of species i.

Energy Transport

Usually, the coating is heated by hot air blown on the top and the bottom sides. In the present work, heat transfer occurs due to natural convection only as experiments were made under quiescent conditions. Because coatings are thin, the conductive resistance of the coating is negligible compared to convective resistance in the air. Hence, the coating temperature was assumed to be uniform through the thickness.[20] Detailed heat transport model of Price and Cairncross[34] showed insignificant change in temperature from the top to the bottom of the coating. Also, temperatures of the coating and the substrate were assumed to be the same.

The equation for heat transport is given by the following equation:

$$\frac{dT}{dt} = -\left[\frac{h_{\text{top}}(T-T^G) + \sum_{i=1}^{N-1}k_{gi}^G\Delta\hat{H}_{vi}\left(p_{ii}^G - p_{ib}^G\right) + h_{\text{bottom}}(T-T^g)}{\rho^p\hat{C}_p^pX(t) + \rho^s\hat{C}_p^sH}\right] \tag{40}$$

h_{top} and h_{bottom} are the heat transfer coefficients on the top and the bottom sides, respectively. $\Delta\hat{H}_{vi}$, is the enthalpy of evaporation of solvent i, ρ, is the density,

$\hat{C}_p$ is the specific heat, superscripts, p and s stand for the polymer and the substrate, respectively.

Solution of Equations

Equations (25) and (26) are partial differential equations, and eqs. (33) and (40) are ordinary differential equations; all these equations are coupled and nonlinear. Together they model the mass and heat transport during drying. Galerkin's method of finite elements is used to transform the partial differential equations into ordinary differential equations (ODEs). The method is described below.

Galerkin's Method of Finite Elements. In this method, concentrations are expressed as a sum of product of unknown coefficients and basis functions:

$$c_1 = \sum_{j=1}^{n} u_j\phi_j \tag{41}$$

$$c_2 = \sum_{j=1}^{n} v_j\phi_j \tag{42}$$

ϕ_j are basis functions, n is number of nodes in the domain at which the solution is computed and u_j and v_j are unknown coefficients. The basis functions, ϕ_j, are chosen such that they have a value of 1 at node j and 0 at others. This choice of the basis functions renders the computed coefficients, u_j and v_j, as solution at the nodes. The functions are usually piece-wise continuous polynomials of a certain degree because they lend

themselves to easy integration.[35] Equations (41) and (42) are differentiated with respect to t and z and substituted into the governing partial differential eqs. (25) and (26). The residuals of the eqs. (25) and (26) are made orthogonal to all functions taken from a complete set of infinite number of independent functions. For practical purposes, however, finite numbers of functions, as warranted by a trade-off between accuracy and computation time, are taken from the set.

Residuals of the eqs. (25) and (26) obtained after substituting the derivatives of c_1 and c_2 with respect to t and z are:

$$R_1 = \int_0^L \left(\sum_{j=1}^{n} \frac{\partial u_j}{\partial t}\phi_j\right)\psi_i dz - \int_0^L \left[\frac{\partial}{\partial z}\left(D_{11}\sum_{j=1}^{n} u_j \frac{\partial \phi_j}{\partial z}\right)\right]\psi_i dz - \int_0^L \left[\frac{\partial}{\partial z}\left(D_{12}\sum_{j=1}^{n} v_j \frac{\partial \phi_j}{\partial z}\right)\right]\psi_i dz \quad (43)$$

$$R_2 = \int_0^L \left[\sum_{j=1}^{n} \frac{\partial v_j}{\partial t}\phi_j\right]\psi_i dz - \int_0^L \left[\frac{\partial}{\partial z}\left(D_{21}\sum_{j=1}^{n} u_j \frac{\partial \phi_j}{\partial z}\right)\right]\psi_i dz - \int_0^L \left[\frac{\partial}{\partial z}\left(D_{22}\sum_{j=1}^{n} v_j \frac{\partial \phi_j}{\partial z}\right)\right]\psi_i dz \quad (44)$$

For each i ($i = 1,n$), one ODE is obtained for eq. (43) and one for eq. (44). The total number of ODEs thus generated are $2\ n$. These ODEs can be represented in a matrix form as

$$A\ \dot{U} = B\ U + C \quad (45)$$

A is a matrix of size $2\ n \times 2\ n$ containing the first term of eqs. (43) and (44). $\dot{U}$ is a vector of time derivatives of the concentrations of solvent 1 and 2 at all the locations. U is vector of the concentrations of solvent 1 and 2. B is a matrix of size $2\ n \times 2\ n$ containing the second and third terms of eqs. (43) and (44). C is a vector ($2\ n \times 1$) containing only two nonzero elements, which are the boundary conditions for eqs. (25) and (26).

In Galerkin's method, the functions, ψ_j are chosen to be same as the basis functions, ϕ_j. In this work, the basis functions were chosen to be quadratic polynomials. For these polynomials, each element has three nodes—one at each end and the third one at the centre. The total number of locations at which concentrations are found is $n = 2n_e + 1$ where n_e = number of elements. The coating thickness was divided into n_e elements, at all instants of time. The elements were made nonuniform with their size rising gradually from the top to the bottom. The elements near the top were chosen to be small to capture the precipitous drop in concentration there. A benefit of using nonuniform elements is reduction in computation time. A function, $r_i = \left(\frac{i-1}{n_e}\right)^2 L$, where i varies from 1 to $n_e + 1$ stretched the elements from the top to the bottom of the coating. The size of element i can be obtained by $r_{i+1} - r_i$. The exponent in the stretching function can be changed to raise or lower stretching.

Matrices A and B are computed and then the eq. (45) is expanded to generate $2\ n$ ODEs. To these ODEs, eqs. (33) and (40) are appended to produce a total of $2\ n + 2$ ODEs. The set of ordinary differential equations generated by expanding eq. (45) was integrated by a stiff solver, *ode15s*, of MATLAB. 50 elements were taken in the present study; doubling the number to 100 changed the concentrations at all locations by <1%. A typical run on a 2.66 GHz computer with a memory of 506 MB took about 20 s. The code was tested with published results[20] and a good comparison was obtained.

Estimation of Free Volume Parameters

Different researchers[20,36–38] reported different values for D_{01} and $\frac{K_{11}}{\gamma}$ for polystyrene–toluene system. Vrentas and Chu[38] studied the effect of polymer molecular weight on D_{01} and its magnitude increases with decrease in molecular weight of polymer because of small jumping unit. Vrentas and Duda[39] have studied the effect of solvent weight fraction on D_{01} and results indicates that its value increases by several order of magnitude with increase in solvent weight fraction.

Therefore, it was considered necessary to estimate the free volume parameters for each of the two systems studied. Price et al.[40] mentioned that out of the nine parameters (D_0, E, ξ, $\frac{K_{11}}{\gamma}$, $K_{21} - T_{gs}$, $\frac{K_{12}}{\gamma}$, $K_{22} - T_{gp}$, $\widehat{V}_s^*$, $\widehat{V}_p^*$) required to predict mutual diffusion coefficient of a binary polymer solvent system, five (E, $\frac{K_{11}}{\gamma}$, $K_{21} - T_{gs}$, $\widehat{V}_p^*$, and $\widehat{V}_s^*$) can be calculated from the pure substance properties and the remaining four parameters, D_0, ξ, $\frac{K_{12}}{\gamma}$ and $K_{22} - T_{g2}$ can be estimated from drying experiments. They estimated these four parameters by minimizing the difference between experimental weight loss measurements with predicted ones.

The four free volume parameters were estimated along same lines as Price et al.[40] A code for drying of binary polymer solvent systems was written and used to generate residual solvent as a function of time. Weight loss data were collected for four polymer–solvent pairs, poly(styrene)-tetrahydrofuran, poly(styrene)-*p*-xylene, poly(methyl methacrylate)-ethylbenzene and poly(methyl methacrylate)- tetrahydrofuran at room temperature and quiescent conditions. The difference between experimental and predicted residual solvent, defined here as an objective function, was minimized by using a built-in optimization code, *lsqnonlin*, of MATLAB. These are listed in Table III for the four pairs.

RESULTS AND DISCUSSION

Figures 8–10 show comparison of model predictions and experimental measurements of concentrations of tetrahydrofuran, *p*-xylene and poly(styrene) at several depths from the base of the coating in a ternary coating as a function of time. As drying progressed, the measurements were made deeper in the coating. The initial thickness of the coating was about 1004 μm, the initial concentrations of the components listed in the same order as above were 0.63 g cm^{-3}, 0.14 g cm^{-3}, and 0.13 g cm^{-3}, respectively, and the drying temperature was 23°C. Figure 8 shows that all the theories predict the concentration of tetrahydrofuran well. Its concentration falls rapidly during the initial stages of drying because it is highly volatile; at later stages, its concentration plateaus off at a low value.

Table III. Free Volume Parameters of Four Binary Polymer Solvent Systems

Parameter	Unit	PS(3)/ THF(2)	PS(3) / *p*-xylene(1)	PMMA(3)/ THF(2)	PMMA(3)/ EB(1)
D_0	$\frac{cm^2}{s}$	**97.99×10^{-4}**	**78.44×10^{-4}**	**98.75×10^{-4}**	**4.11×10^{-4}**
$\frac{K_{13}}{\gamma}$	$\frac{cm^3}{g.K}$	**2.89×10^{-4}**	**2.89×10^{-4}**	**5.89×10^{-4}**	**5.89×10^{-4}**
K_{23}	K	**−326.46**	**−326.46**	**−230.44**	**−230.44**
ξ		**0.38**	**0.44**	**0.65**	**0.30**
K_{2i}	K	10.45	41.65	10.45	−80.01
$\frac{K_{1i}}{\gamma}$	$\frac{cm^3}{g.K}$	7.53×10^{-4}	7.6×10^{-4}	7.53×10^{-4}	2.22×10^{-3}
$\hat{V}*$	$cm^3\ g^{-1}$	0.899	1.049	0.899	0.946
$\hat{V}*$	$cm^3\ g^{-1}$	0.855	0.855	0.788	0.788
χ_{i3}		0.3652	0.5429	0.3925	0.3501
χ_{12}		0.4371	0.4371	0.4188	0.4188

The values shown in bold face were obtained from optimization. The values of other parameters were obtained from literature.[9]

Solvents Properties/Coefficients
- Enthalpy of vaporization of tetrahydrofuran: 413.53 J g^{-1}
- Enthalpy of vaporization of *p*-xylene:335.98 J g^{-1}
- Enthalpy of vaporization of ethylbenzene: 335.03 J g^{-1}
- Mass transfer coefficient of tetrahydrofuran: 1.74×10^{-9} s cm^{-1}
- Mass transfer coefficient of *p*-xylene:1.92×10^{-9} s cm^{-1}
- Mass Transfer coefficient of ethylbenzene: 1.92×10^{-9} s cm^{-1}

Substrate Properties
- Thickness of sample holder: 0.15 cm
- Density of sample holder: 8 g cm^{-3}
- Specific heat capacity of substrate: 0.5 J g^{-1} K^{-1}
- Thermal conductivity of substrate: 0.162 W cm^{-1} K^{-1}

Polymer Properties
- Specific heat capacity of poly (styrene): 1.17 J g^{-1} K^{-1}
- Specific heat capacity of poly (methyl methacrylate): 1.5 J g^{-1} K^{-1}

Figure 9 shows that the concentration of *p*-xylene rises from its initial value at 400, 300, and 200 μm from the base of the coating. In the beginning, tetrahydrofuran leaves the coating sooner than *p*-xylene because of higher volatility. This leads to an increase in the concentration of *p*-xylene; in fact, model predictions show that the increase is found at all locations in the coating. Later, when the concentration of tetrahydrofuran plateaus, concentration of *p*-xylene falls everywhere in the coating. Predictions of all theories are in good agreement with measurements in the initial stages when drying is dominated by the external mass transfer coefficient. In the later stages, drying is influenced by internal diffusion and, the theories seem to over-predict the concentration. Generalized model predictions are better than others; theories with cross term coefficients included, Zielinski and Hanley's, Case 1 of Alsoy Duda's appear to predict better than those that neglect them. This is in keeping with the results of Zielinski and Alsoy.[22]

Alsoy and Duda[20] compared predictions of drying model which utilizes several of their theories for diffusion coefficients with experimental weight loss data of Drake and Wang.[41] It is worth noting that during later stages of drying, their model over-predicts the data for all the theories. This seems to be due to over-prediction of less volatile component as shown in Figure 9.

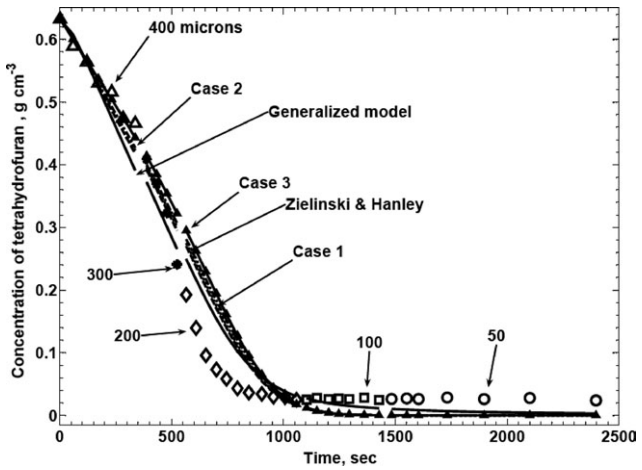

Figure 8. Concentration of tetrahydrofuran at several locations from the base as a function of time for poly (styrene)–tetrahydrofuran–*p*-xylene system. Initial concentration of poly (styrene), tetrahydrofuran and *p*-xylene were 0.1277, 0.6324 and 0.1414 g cm^{-3}, initial coating thickness was 1004 μm and initial temperature of coating and air was 23°C.

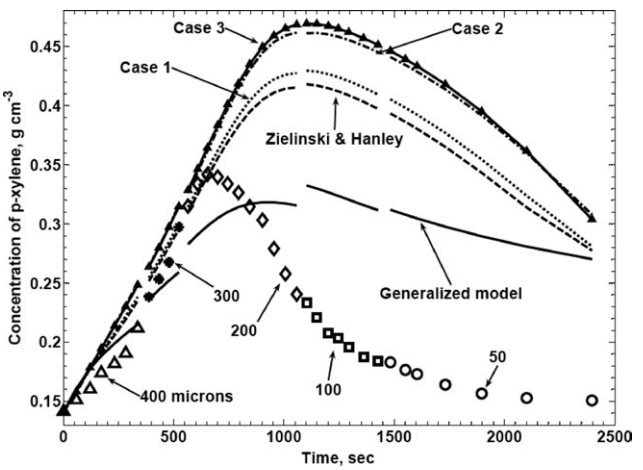

Figure 9. Concentration of *p*-xylene at several locations from the base as a function of time for poly (styrene)–tetrahydrofuran–*p*-xylene system. Initial concentration of poly (styrene), tetrahydrofuran and *p*-xylene were 0.1277, 0.6324 and 0.1414 g cm^{-3}, respectively. Initial coating thickness was 1004 μm and temperatures of coating and air were 23°C.

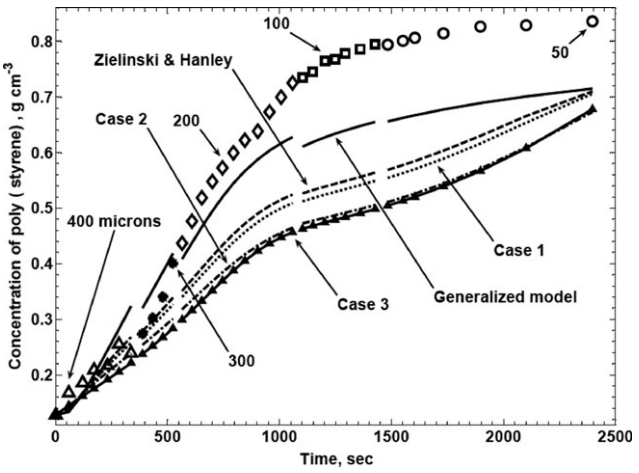

Figure 10. Concentration of poly (styrene) at several locations from the base as a function of time for poly (styrene)–tetrahydrofuran–*p*-xylene system. Initial concentrations of poly (styrene), tetrahydrofuran and *p*-xylene were 0.1277, 0.6324, and 0.1414 g cm^{-3}, respectively. Initial coating thickness was 1004 μm and temperatures of coating and air were 23°C.

The discrepancy between predictions and experiments is more during later stages of drying when most of the tetrahydrofuran is removed. This suggests that presence of even small amounts of tetrahydrofuran effects removal rates of *p*-xylene. The contribution of cross-term factor that drives *p*-xylene transport due to concentration gradient of tetrahydrofuran is significantly high. Other possible reasons for the difference could be attributed to thermodynamics of polymer solvent systems as mentioned by Price et al.[40]

Poly (styrene) is expected to go through glass transition during drying, especially near the top of the coating, because the drying temperature is 23°C and glass transition temperature is about 100°C. Free volume theory under predicts the diffusion coefficients of polymer solvent systems which go through glass transition. Hence, the concentrations predicted by the theories for multicomponent diffusion are expected to be higher than measurements. There are few reports on measurements of diffusion coefficients of binary polymer solvent systems in the glassy region. For the binary pairs studied here, no data is available; for ternary systems, the glass transition of polymer solvent system is determined by the concentrations of both the solvents. Hence, it was difficult to incorporate the rise in diffusion coefficients in the glassy region.

Figure 10 shows that the concentration of poly(styrene) rises in the coating. This is because the solvents depart from the coating and the polymer being highly nonvolatile does not. All the theories appear to under predict the concentration of poly(styrene). Generalized model seems to better than other theories. In general, theories, which include cross-term coefficients (Zielinski and Hanley[18] and Case 1 of Alsoy and Duda[20]) appear to better than those that do not. During the experiments, the laser was focused at a certain depth in the coating through the air between the objective and the coating.

Figure 11 shows measurements of coating thickness and the ratio of depth of position at which measurements were made to instantaneous coating thickness as a function of time for poly(-styrene)–tetrahydrofuran–*p*-xylene coating. The ratio was always greater than 0.3, which means the measurements were not made close the top surface where significant concentration gradients can be expected.

Figure 12 shows the comparison of experimental coating thickness with the model predictions. None of model is able to predict the experimental behavior of coating thickness in case of poly(styrene)–tetrahydrofuran–*p*-xylene system.

Figures 13–15 show comparison of measurements of concentration of ethyl benzene, tetrahydrofuran, and poly(methyl methacrylate) and predictions of different models. The measurements were made at several depths in the coating at different times. Initial concentration of poly(methyl methacrylate), tetrahydrofuran,

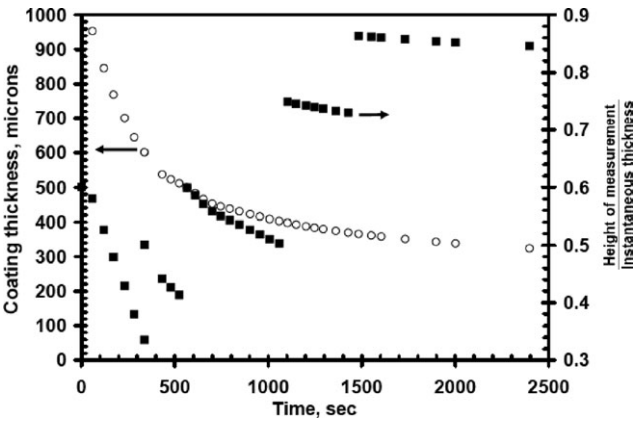

Figure 11. Change in coating thickness with time for poly (styrene)–tetrahydrofuran–*p*-xylene system. Initial concentrations of poly (styrene), tetrahydrofuran, and *p*-xylene were 0.1277, 0.6324, and 0.1414 g cm^{-3}, respectively. Initial coating thickness was 1004 μm and initial temperatures of coating and air were 23°C.

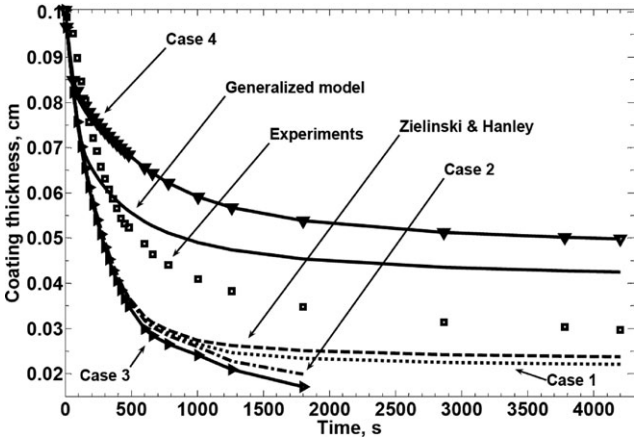

Figure 12. Coating thickness as a function of time for poly (styrene)–tetrahydrofuran–*p*-xylene system. Initial concentration of poly (styrene), tetrahydrofuran and *p*-xylene were 0.1277, 0.6324, and 0.1414 g cm^{-3}, initial coating thickness was 1004 μm and initial temperature of coating and air was 23°C.

Applied Polymer SCIENCE

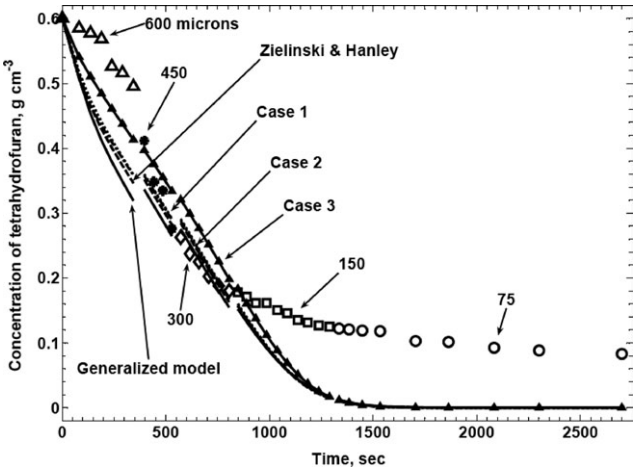

Figure 13. Concentration of tetrahydrofuran at several locations from the base as a function of time for poly (methyl methacrylate)–tetrahydrofuran–ethylbenzene system. Initial concentrations of poly (methyl methacrylate), tetrahydrofuran and ethylbenzene were 0.2157, 0.6003, and 0.1219 g cm^{-3}, respectively. Initial coating thickness was 983 μm and initial temperatures of coating and air were 23°C.

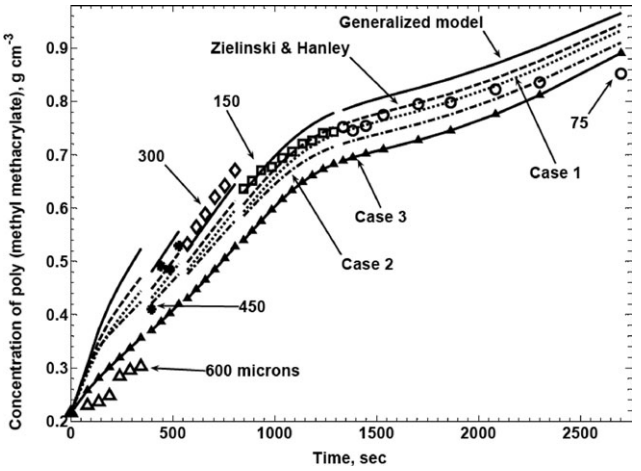

Figure 15. Concentration of poly (methyl methacrylate) at several locations from the base as a function of time for poly (methyl methacrylate)–tetrahydrofuran–ethylbenzene system. Initial concentrations of poly (methyl methacrylate), tetrahydrofuran, and ethylbenzene were 0.2157, 0.6003, and 0.1219 g cm^{-3}, respectively. Initial coating thickness was 983 μm and initial temperatures of coating and air were 23°C.

and ethylbenzene were, 0.2157, 0.6003, and 0.1219 g cm^{-3}, respectively. Initial thickness of the coating was 983 μm.

All the models seem to predict concentrations of the solvents and the polymer reasonably well during the initial stages of drying. But, in the later stages, they seem to under-predict concentration of tetrahydrofuran and over-predict concentration of ethylbenzene. Predictions of the models that have cross-term diffusion coefficients included appear to better than those that do not. For the two systems studied here, the models are conservative in that they predict higher concentration of less volatile solvent. Hence, the residual solvent predicted by them would be higher.

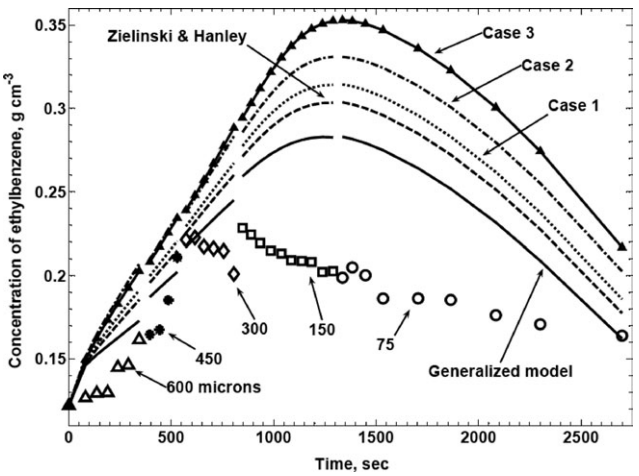

Figure 14. Concentration of ethylbenzene at several locations from the base as a function of time for poly (methyl methacrylate)–tetrahydrofuran–ethylbenzene system. Initial concentrations of poly (methyl methacrylate), tetrahydrofuran and ethylbenzene were 0.2157, 0.6003, and 0.1219 g cm^{-3}, respectively. Initial coating thickness was 983 μm and initial temperatures of coating and air were 23°C.

The ratio of depth of position at which concentrations were measured to the instantaneous coating thickness was at least 0.2 which is shown in Figure 16. At these depths, steep concentration gradients are not expected. Hence, the effect of mismatch between actual and set depths of focus on measurements is negligible. All the models are under predicting the coating thickness as shown in Figure 17.

CONCLUSIONS

This paper presented experimental measurements of concentrations of ternary polymer solvent systems comprising a polymer and two solvents by confocal laser Raman spectroscopy. Concentrations of the solvents were measured for two ternary

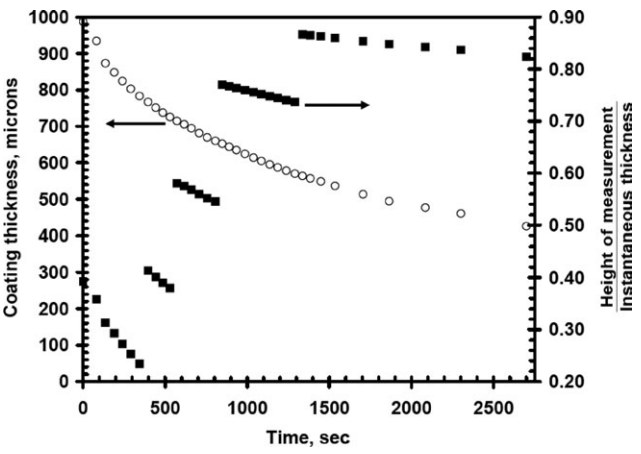

Figure 16. Change in coating thickness for poly (methyl methacrylate)–tetrahydrofuran–ethylbenzene system. Initial concentrations of poly (methyl methacrylate), tetrahydrofuran, and ethylbenzene were 0.2157, 0.6003, and 0.1219 g cm^{-3}, respectively. Initial coating thickness was 1004 and initial temperatures of coating and air were 23°C.

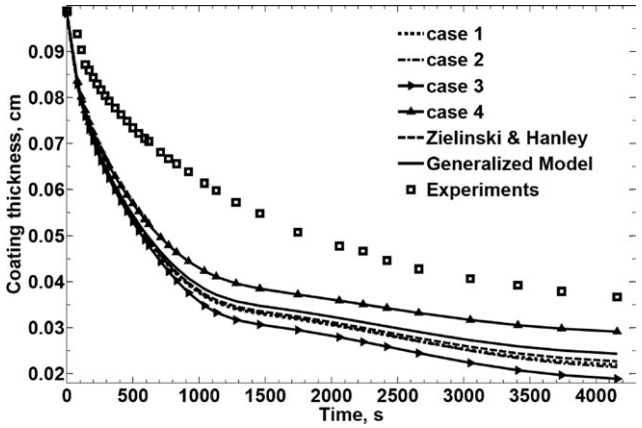

Figure 17. Coating thickness as a function of time for poly (methyl methacrylate)–tetrahydrofuran–ethylbenzene system. Initial concentrations of poly (methyl methacrylate), tetrahydrofuran, and ethylbenzene were 0.2157, 0.6003, and 0.1219 g cm^{-3}, respectively. Initial coating thickness was 983 μm and initial temperatures of coating and air were 23°C.

systems, poly(styrene)–tetrahydrofuran–*p*-xylene and poly(-methyl methacrylate)–ethylbenzene–tetrahydrofuran, during drying at room temperature. They were compared with predictions of a drying model, which utilizes several existing theories for mutual diffusion coefficients for polymer solvent systems. Of the nine free volume parameters required to predict diffusion coefficients of binary systems, four for each of the four pairs studied here were estimated as suggested by the literature. Estimation was done by minimizing the difference between predictions of the model and experimental weight loss data for each binary pair.

All the theories appear to predict the concentration of more volatile component well but over-predict the concentration of less volatile component. The concentration of this component goes through a maximum during drying.

ACKNOWLEDGMENTS

Authors are very much thankful to Prof. D. S. Misra, Department of Physics, IIT Bombay, for permitting use of confocal Raman spectroscopy facility. Authors are also thankful to Mrs. Sharlet Joseph, Superintendant of the facility for performing timely analysis of coatings.

REFERENCES

1. Dabral, M.; Francis, L. F.; Scriven, L. E. *AIChE J.* **2002**, *48*, 25.
2. Kesting, R. E. Synthetic Polymeric Membranes—A Structural Perspective; Wiley-Interscience: New York, **1985**.
3. Mulder, M. H. V. Membrane Science and Technology Series, 1(Pervaporation Membr. Sep. Processes), **1991**, 225.
4. Koros, W. J.; Pinnau, I. Membrane Formation for Gas Separation Processes, Polymeric Gas Separation Membranes, CRC Press: Boca Raton, **1994**, p 209.
5. Shojaie, S. S.; Krantz, W. B.; Greenberg, A. R. *J. Membr. Sci.* **1994**, *94*, 255.
6. Shojaie, S. S.; Krantz, W. B.; Greenberg, A. R. *J. Membr. Sci.* **1994**, *94*, 281.
7. Vrentas, J. S.; Duda, J. L. *J. Polym. Sci.: Polym. Phys. Ed.* **1977**, *15*, 403.
8. Vrentas, J. S.; Duda, J. L. *J. Polym. Sci.: Polym. Phys. Ed.* **1977**, *15*, 417.
9. Hong, S. *Ind. Eng. Chem. Res.* **1995**, *34*, 2536.
10. Yapel, R. A. The Physical Model of Drying of Coated Films, M. S. Thesis, University of Minnesota, Minneapolis, USA, **1988**.
11. Alsoy, S.; Duda, J. L. *Drying Tech.* **1998**, *16*, 15.
12. Alsoy, S. *Ind. Eng. Chem. Res.* **2001**, *40*, 2995.
13. Schabel, W.; Scharfer, P.; Mueller, M.; Ludwig, I.; Kind, M. *Chemie Ingenieur Technik* **2003**, *75*, 1336.
14. Onsager, L. *Phys. Rev.* **1931**, *38*, 2265.
15. DeGroot, S. R.; Mazur, P. Non-Equilibrium Thermodynamics; North-Holland Pub: Amsterdam, **1962**.
16. Cussler, E. L. Multicomponent Diffusion; Elsevier Scientific Pub.: Amsterdam, Netherlands, **1976**.
17. Bearman, R. J. *J. Phys. Chem.* **1961**, *65*, 1961.
18. Zielinski, J. M.; Hanley, B. F. *AIChE J.* **1999**, *45*, 1.
19. Dabral, M. Solidification of coatings: theory and modeling of drying, curing and microstructure growth, Ph.D. Thesis, University of Minnesota, Minneapolis, MN, USA,**1999**.
20. Alsoy, S.; Duda, J. L. *AIChE J.* **1999**, *45*, 896.
21. Alsoy, S. Modeling of Polymer Drying and Devolatilization Processes, Ph.D. Thesis, Pennsylvania State Univ., USA, **1998**.
22. Zielinski, J. M.; Alsoy, S. *J. Polym. Sci. Part B: Polym. Phys.* **2001**, *39*, 1496.
23. Nauman, E. B.; Savoca, J. *AIChE J.* **2001**, *47*, 1016.
24. Price, P. E., Jr.; Romdhane, I. H. *AIChE J.* **2003**, *49*, 309.
25. Surana, R. K.; Danner, R. P.; Duda, J. L. *Ind. Eng. Chem. Res.* **1998**, *37*, 3203.
26. Galdamez, J. R.; Danner, R. P. *Ind. Eng. Chem. Res.* **2009**, *48*, 4966.
27. Muller, M.; Kind, M.; Cairncross, R.; Schabel, W. *Eur. Phys. J. Special Topics* **2009**, *166*, 103.
28. Chow, T. S. *Macromolecules* **1980**, *13*, 362.
29. Arya, R. *Int. J. Chem. Eng. Appl.* **2011**, *2*, 421.
30. Cairncross, R. A. Solidification Phenomena During Drying of Sol-to-Gel Coatings, Ph.D. Thesis, Univ. of Minnesota, Minneapolis, MN, **1994**.
31. Vrentas, J. S.; Duda, J. L.; Ling, H. C. *J. Polym. Sci. Polym. Phys. Ed.* **1984**, *22*, 459.
32. Favre, E.; Nguyen, Q. T.; Clement, R.; Neel, J. *Eur. Polym. J.* **1996**, *32*, 303.
33. Bristow, G. M.; Watson, W. F. *Trans. Faraday Soc.* **1958**, *54*, 1731.

34. Price, P. E., Jr.; Cairncross, R. A. *J. Appl. Polym. Sci.* **2000**, *78*, 149.
35. Strang, G.; Fix, G. J. Analysis of the Finite Element Method; Englewood Cliff, Princeton Hall, Wellesley-Cambridge Press.
36. Duda, J. L.; Vrentas, J. S.; Ju, S. T.; Liu, H. T. *AIChE J.* **1981**, *28*, 279.
37. Vrentas, J. S.; Duda, J. L.; Ling, H. C.; Hou, A. C. *J. Polym. Sci. Polym. Phys. Ed.* **1985**, *23*, 289.
38. Vrentas, J. S.; Chu, C. H. *J. Polym. Sci. Part B: Polym. Phys.* **1989**, *27*, 465.
39. Vrentas, J. S.; Duda, J. L. *J. Polym. Sci. Polym. Phys. Ed.* **1977**, *15*, 441.
40. Price, P. E., Jr.; Wang, S.; Romdhane, I. H. *AIChE J.* **1997**, *43*, 1925.
41. Drake, M. C.; Wang, S. AIChE Meeting, San Francisco, CA, **1989**.